Analyst

RSCPublishing

Supplementary Data

Real-time direct cell concentration and viability determination using a fully automated microfluidic platform for standalone process monitoring

P. S. Nunes,[a] S. Kjaerulff,[b] M. Dufva[a] and K. B. Mogensen[a],

Cite this: DOI: 10.1039/xoxxoooooox

Received ooth January 2015,
Accepted ooth January 2015

DOI: 10.1039/xoxxoooooox

www.rsc.org/

This supplementary data document presents additional details for our research paper regarding: S1 – Chip design and flow simulations; S2 – Experimental setup; S3 – Automated image analysis.

S1: Chip design and flow simulations

Flow simulations

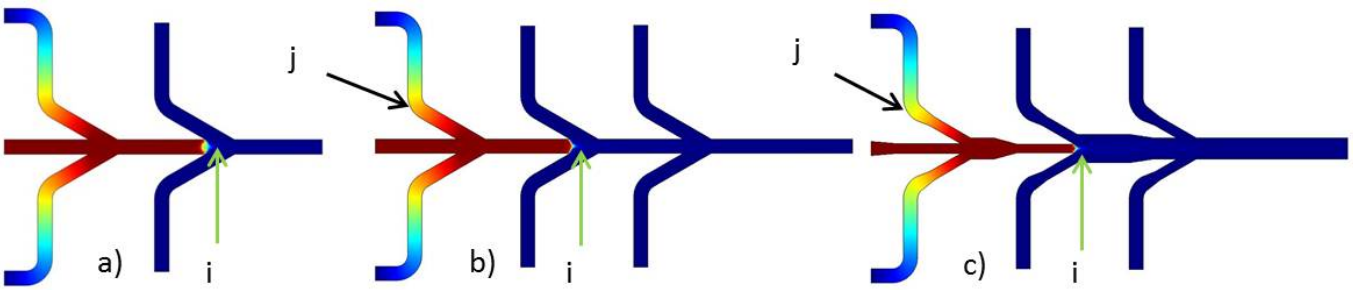

Figure S1 – Comsol simulations of the sample concentration. The red color corresponds to a normalized sample concentration of 1, while the dark blue corresponds to 0. The sample flow rate was 5.5 µl/min, while the washing buffer flow rates was 0 µl/min. a) Diluents flow rate of 708 µl/min per channel. b) Standard channels width 0.5 mm and diluents flow rate of 354 µl/min per channel. c) Restricted channels width and diluents flow rate of 354 µl/min per channel.

Fluidic simulations using the numerical finite element method (FEM) were implemented in Comsol Multiphysics (Comsol 4.3b, Comsol AB, Sweden), as previously described.

Performing large dilutions with the current method of individually adjusting the flow rates of the sample and of the diluent creates large differences in the necessary flow rates, which may lead to high backpressures. This could prevent the cells from being diluted, or contaminate the surrounding channels with foreign species. Figure S1 a) and b) illustrates that when the flow rates are significantly different, there is a backflow in the central channel (marked with i), which leads to an increase in the expected dilution factor.

Therefore the final microfluidic device consists of four inlet channels for the dilution buffer connected to the central channel on both sides.

The microfluidic chip is intended as a multiple-use device, so the channels geometries were designed to facilitate the cleaning of the chip, as well as to prevent foreign species from entering the surrounding channels. By reducing the width of the inlet channels, the fluidic resistance can be increased, thus preventing species from entering the surrounding channels, marked with j in Figure S1 b) and c). The final design consisted of a 0.350 mm restriction in comparison to the initial 0.5 mm wide channel, which was motivated by the preference to use the same milling tool used to fabricate the microfluidic chips middle layer.

Chip design

The components fabricated were designed in SolidWorks (Version SP4.0, 2012, Dassault Systemes, USA). SolidCam (Version SP6, 2012, SolidCam, USA) integrated with SolidWorks was used as computer aided manufacturing (CAM) engine, enabling the designs to be CNC micromilled. The microfluidic chip middle layer was designed with different channel widths in the points where different fluids merge, as can be seen in Figure S2, while maintaining a constant depth (0.5 mm).

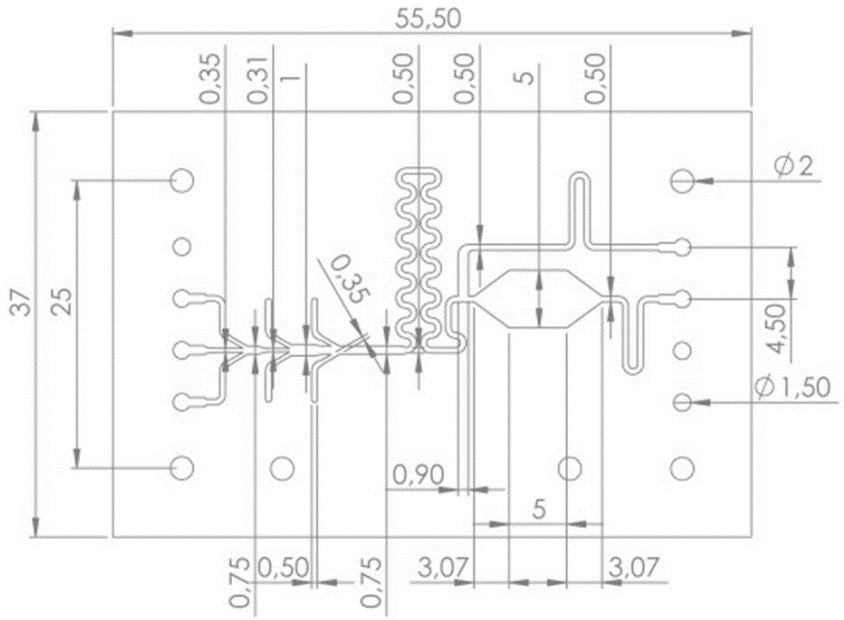

Figure S2 - Schematic of the microfluidic chip middle layer and respective dimensions (mm).

To ensure that there is no collapse of the chamber lid after bonding, the chamber depth was also determined by measuring the absorbance of a 1 mM aqueous solution of bromothymol blue in the chamber using a spectrophotometer (UV-1800, Shimadzu, Japan). Bromothymol blue in Milli-Q water (1mM) was injected into the microfluidic chip, and the absorbance in the imaging area measured (Abs_{chipBB}). In order to eliminate other optical interference sources (e.g.: surface roughness) a reference measurement was also performed by filling the chip with Milli-Q water (Abs_{chipH_2O}). To eliminate the absorptivity ε from Lambert-Beer's law the absorbances of 0.1 mM Bromothymol blue and Milli-Q water were measured in a cuvette with a well-defined length (L_{cuv} = 5 mm), Abs_{cuvBB} and Abs_{cuvH_2O}, respectively.

$$\frac{Abs_{chipBB} - Abs_{chipH_2O}}{Abs_{cuvBB} - Abs_{cuvH_2O}} = \frac{c_{chipBB} \times L_{chip} \times \varepsilon}{c_{cuvBB} \times L_{cuv} \times \varepsilon}$$

To ensure that the measured absorbance was corresponding always to the same area in the imaging chamber, a holder was fabricated in blue PMMA (5 mm thick) using the CO2 laser. The holder could be aligned directly with the through holes present in the chip corners, and with the cuvette holder fixed in the spectrophotometer. Results showed that the chamber depth after bonding was the same as measured with the profilometer.

S2: Experimental setup

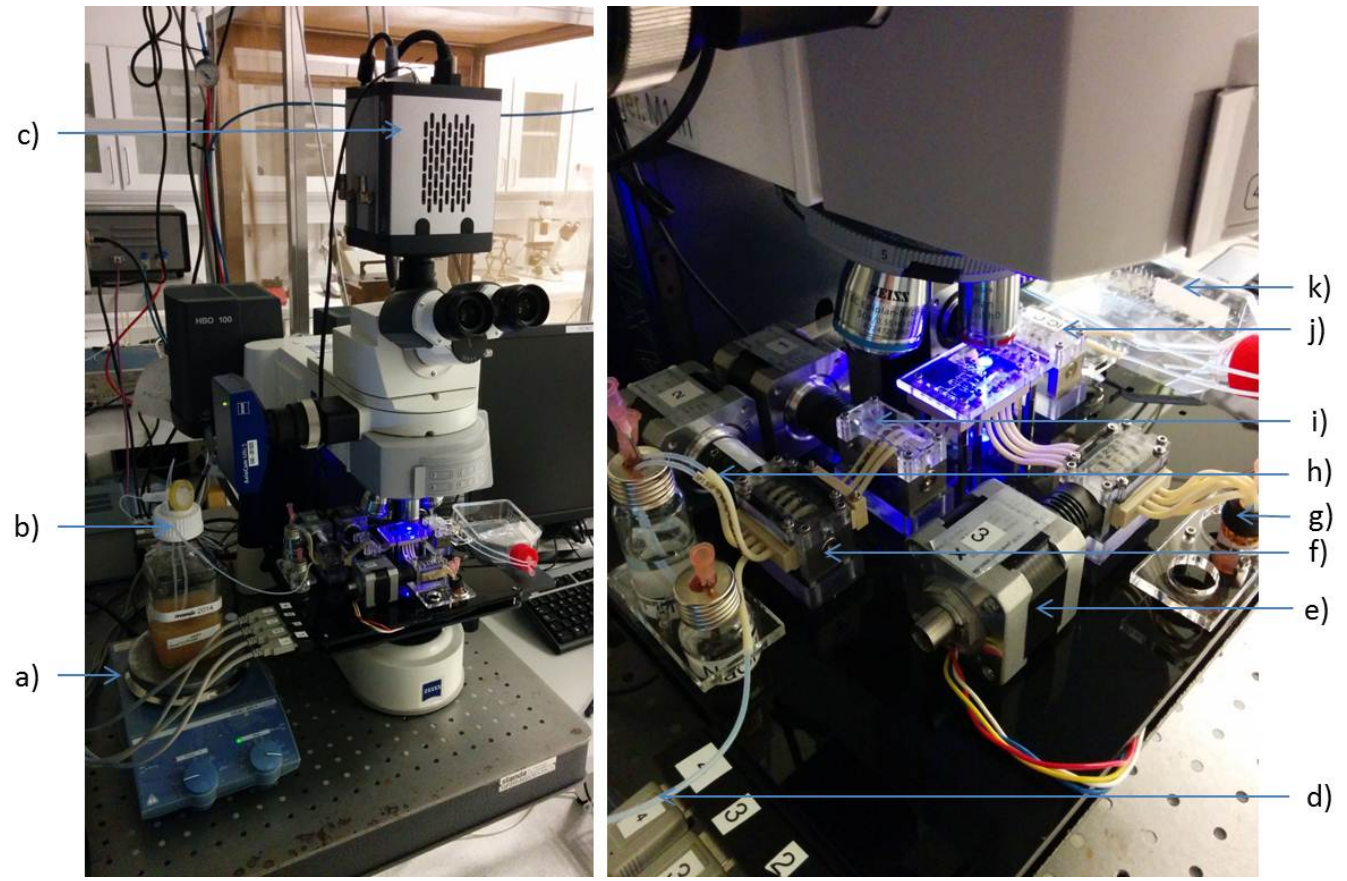

Figure S3 – Setup for monitoring in real-time the concentration and viability of yeast cells during fermentation consisting of: a) magnetic stirrer, b) home-made bioreactor, c) camera and trigger cable for image acquisition, d) tube connecting the bioreactor to the multi-channel peristaltic pump, e) stepper motor controlling the peristaltic pump driving the staining and dilution buffer, f) peristaltic pump driving the cleaning buffer (0.1 M NaOH) and the cell sample, g) staining and dilution buffer, h) cleaning buffer (0.1 M NaOH), i) multi-channel valve, j) multi-channel outlet valve, k) waste reservoir.

Supplementary Data

S2: Automated image analysis

In order to validate the brightfield and fluorescence image analysis programs, the chambers of 12 nucleocassettes were imaged using a Zeiss microscope. The concentration and viability values obtained from the NC3000, provided by ChemoMetec, can then be directly compared with the values calculated using Matlab. In this way, it is possible to get an accurate assessment of the image analysis performance, independently of fluid manipulations and the quality of the imaging surface.

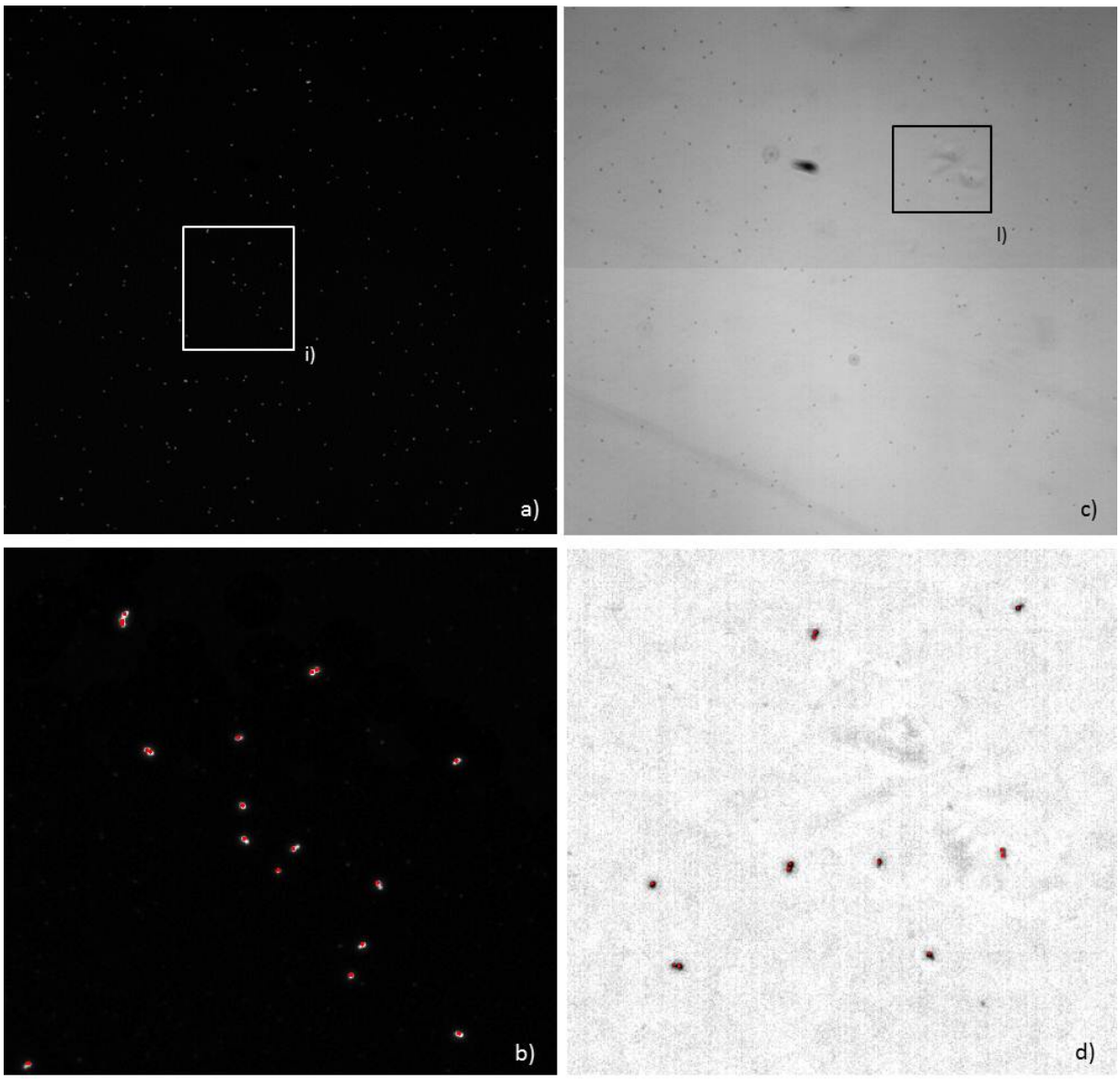

Figure S4 – Image analysis of: a) Fluorescence image of PI stained cells in the Nucleocassete obtained in the Zeiss microscope (5x magnification, imaged area: 2,64 mm x 2,77 mm), b) Close-up of insert i) after running the automated image analysis program CellAuto, 24 individual cells are marked with a red dot in the imaged area (0,62 mm x 0,55 mm), c) Brightfield image of PI stained cells in the Nucleocassete obtained in the Zeiss microscope (imaged area: 2,64 mm x 2,77 mm) and d) Close-up of insert l) after running the automated image analysis program CellAuto for brightfield images, 12 individual cells are marked with a red dot in the Imaged area (0,46 mm x 0,49 mm).

Image analysis was performed using a program written in Matlab, based on further modified version of the available Image-based tool for counting Nuclei (ITCN). The ITCN is able to quite accurately analyse fluorescence images. However the basic code was further modified by increasing the contrast of the images and subtracting their background, in order to eliminate the inhomogeneity of the halogen light source. Figure S4 a-b) corresponds to the PI stained cells in the NucleoCassete imaged in the Zeiss microscope. Besides counting all the bright spots it is equally important to distinguish individual cells which are clustered as can be seen in Figure S4 b).

Brightfield image analysis poses more challenges as defects in the chamber bottom, or dust particles in the optical system can be interpreted as cells by the automated image analysis program. Therefore, cells are identified in the images by using a size filter and an additional intensity filter, in order to filter surrounding debris. The insert in Figure S4 c) corresponds an area where a clear surface deformation is present. The developed automated program is capable of removing those large structures, but once the contrast of the image is increased, then previously not seen dark spots are clearly identifiable. By applying an intensity filter, these spikes are ignored from the cell count as can be seen in Figure S4 d).

Notes and references

[a] Technical University of Denmark, Department for micro- and nanotechnology, Denmark. E-mail: paro@nanotech.dtu.dk

[b] ChemoMetec A/S, Denmark.